

Selective Inhibitors of Histone Deacetylase 10: Hydrogen Bonding to the Gatekeeper Residue is Implicated

Magalie Géraldy^{1,#}, Michael Morgen¹, Peter Sehr², Raphael R. Steimbach^{1,3}, Johannes Ridinger^{3,4,5,6}, Ina Oehme^{4,5,7}, Olaf Witt^{4,5,6,7}, Mona Malz¹, Mauro S. Nogueira⁸, Oliver Koch⁸, Nikolas Gunkel^{1,7}, Aubry K. Miller^{1,7,*}

¹ Cancer Drug Development Group, German Cancer Research Center (DKFZ), 69120 Heidelberg, Germany

² Chemical Biology Core Facility, European Molecular Biology Laboratory, 69117 Heidelberg, Germany

³ Biosciences Faculty, University of Heidelberg, 69120 Heidelberg, Germany

⁴ Hopp Children's Cancer Center Heidelberg (KITZ), 69120 Heidelberg, Germany

⁵ Clinical Cooperation Unit Pediatric Oncology, German Cancer Research Center (DKFZ), 69120 Heidelberg, Germany

⁶ Department of Pediatric Oncology, Hematology and Immunology, University Hospital Heidelberg, 69120 Heidelberg, Germany.

⁷ German Cancer Consortium (DKTK), 69120 Heidelberg, Germany

⁸ Faculty of Chemistry and Chemical Biology, TU Dortmund University, 44227 Dortmund, Germany

ABSTRACT: The discovery of isozyme-selective histone deacetylase (HDAC) inhibitors is critical for understanding the biological functions of individual HDACs and for validating HDACs as clinical drug targets. The isozyme HDAC10 contributes to chemotherapy resistance via inhibition of autophagic flux and has recently been described to be a polyamine deacetylase, but no studies directed toward selective HDAC10 inhibitors have been published. Herein, we disclose that the use of two complementary ligand-displacement assays has revealed unexpectedly potent HDAC10 binding of tubastatin A, which has been previously described as a highly selective HDAC6 inhibitor. We synthesized a targeted selection of tubastatin A derivatives and found that a basic amine in the cap group was required for strong HDAC10, but not HDAC6, binding. Only potent HDAC10 binders mimicked HDAC10 knockdown by causing dose-dependent accumulation of acidic vesicles in the BE(2)-C neuroblastoma cell line. Docking of inhibitors into human HDAC10 homology models indicated that a hydrogen-bond between a basic cap group nitrogen and the HDAC10 gatekeeper residue Glu272 was responsible for potent HDAC10 binding. Taken together, the presented assays and homology models provide an optimal platform for the development of HDAC10-selective inhibitors, as exemplified with the tubastatin A scaffold.

INTRODUCTION:

The discovery of histone deacetylase 1 (HDAC1) by Taunton and Schreiber in 1996¹ provided the long sought-after enzyme target for substances like trichostatin A (TSA (**1**), Figure 1) and suberanilohydroxamic acid (SAHA (**2**)). At the time, **1** and **2** were reported to increase histone lysine acetylation levels, thereby inducing cellular differentiation, but their mechanism(s) of action were unknown.² Taunton and Schreiber's disclosure launched a now two-decade's long effort to discover inhibitors of HDACs, currently a family of 18 functionally related isozymes.³⁻⁴ During this time it has also become clear that HDACs have a broader role than catalyzing the hydrolysis of acetylated histone lysines: not only do they act in both the nucleus and the cytoplasm, but they catalyze the removal of *acyl* groups from a variety of different proteins.⁵⁻⁹ The 18 HDACs are grouped into four different classes based on homology to their yeast orthologs as follows: Class I (HDAC1, -2, -3, and -8); Class II, which is subdivided into Class IIA (HDAC4, -5, -7, and -9) and Class IIB (HDAC6 and -10); Class III (sirtuin1-7); and Class IV (HDAC11).¹⁰ While Classes I, IIA-B, and IV are Zn²⁺-dependent amidohydrolases, the Class III sirtuins are mechanistically distinct NAD⁺-dependent enzymes. For this reason, the sirtuins are often considered separately in discussions of "HDAC inhibitors". Currently, there are four HDAC inhibitor drugs approved in the U.S. (**2-5**), one in China (**6**), many other candidates undergoing clinical trials, and dozens of reported inhibitors (Figure 1). The approved drugs are used as anti-cancer agents, but HDAC inhibitors are also investigated in the treatment of autoimmune disorders, and neurodegeneration.³ Clinically used pan-HDAC inhibitor drugs (e.g. **2-5**) can cause severe side effects, caused in part by their lack of selectivity. More isozyme-selective inhibitors are expected to overcome these liabilities and are likely to improve the clinical value of this target class.¹⁰⁻¹¹ Moreover, the development of isozyme-selective chemical probes will be critical to further disentangle the biological role(s) of individual HDAC isozymes.¹² To date, the most significant focus and success in the development of selective inhibitors has been with the Class I enzymes, where selective inhibitors of HDAC1/2, HDAC3, and HDAC8 have been disclosed, and with the Class IIB enzyme HDAC6.³ Far fewer selective inhibitors of the Class IIA, HDAC10 or HDAC11 subtypes have been reported.¹³⁻¹⁷

In 2003, tubacin (**7**) was described as the first selective HDAC6 inhibitor (Figure 1).¹⁸ In the intervening years, many additional HDAC6 inhibitors with good selectivity profiles have been described, the most well-known (besides tubacin) being tubastatin A (**8**).¹⁹ Indeed, both **7** and **8**, along with ACY-738 (**9**)²⁰, are designated as HDAC6 chemical probes in the Chemical Probes Portal.²¹ Most HDAC6-selective inhibitors, like **8** and **9**, achieve selectivity over Class I enzymes by incorporating a relatively bulky phenyl

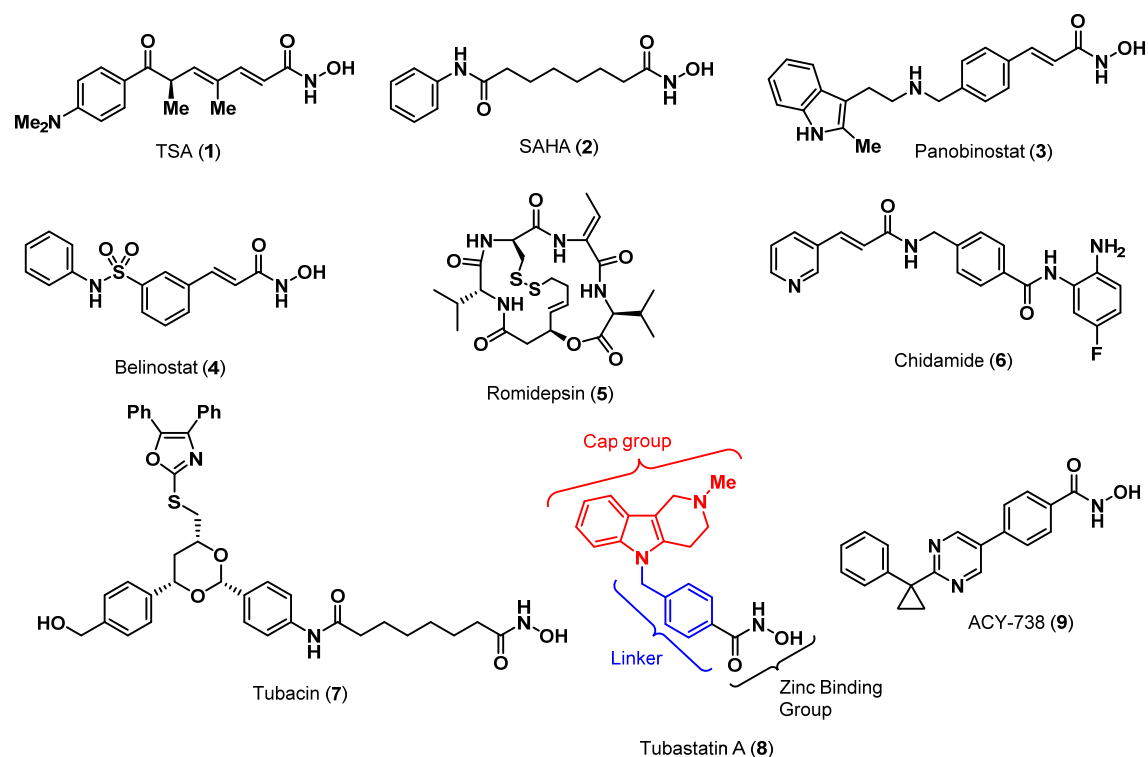


Figure 1: Well-known HDAC inhibitors

hydroxamate “linker” moiety in addition to a “cap group” that can make specific interactions with the HDAC6 protein surface (see 8, Figure 1).

HDAC10 was first isolated in 2002 and annotated as a Class IIB HDAC based on its high similarity to HDAC6.²²⁻²⁴ Like HDAC6, HDAC10 appears to localize to both the nucleus and cytoplasm, and has been reported to interact with proteins having a variety of functions including transcription factors²⁵ and cyclins,²⁶ and to play a prominent role in homologous recombination²⁷ and Hsp-mediated VEGFR regulation.²⁸ While some clinical correlation studies have indicated an apparent tumor-suppressor function for HDAC10,²⁹⁻³³ a number of other studies highlight HDAC10 as a potential cancer drug target.³⁴⁻³⁷ In one study, high HDAC10 expression levels were found to correlate with poor clinical outcome for advanced stage 4 neuroblastoma patients who received chemotherapy.³⁷ Consistent with these findings, HDAC10 depletion in neuroblastoma cells interrupts autophagic flux and sensitizes cells for chemotherapy, and enforced HDAC10 expression protects neuroblastoma cells against doxorubicin treatment.³⁸

Recently, Christianson and co-workers solved the x-ray crystal structure of zebrafish HDAC10 (zHDAC10).⁶ They elegantly demonstrated that both the zebrafish and human HDAC10 (*hHDAC10*) enzymes are highly active polyamine deacetylases (PDAC), while being poor lysine deacetylases.

Therefore, it appears as if HDAC10 may not act on proteins, but on polyamine metabolites, e.g. spermidine and putrescine. Two specific structural features near the active site of the enzyme(s) were identified as being responsible for PDAC activity. First, the negatively charged Glu272 (*h*HDAC10 numbering) amino acid was demonstrated to be a gatekeeper residue, which establishes specificity for cationic polyamine substrates over acetylated lysines. In all other HDAC isozymes except the first catalytic domain of HDAC6, this amino acid is hydrophobic, usually a leucine. Second, the L1 loop of HDAC10 contains a two-residue insertion relative to HDAC6 in both zebrafish and humans. Christianson et al. found that, in *z*HDAC10, these inserted residues plus a two-residue mutation create a unique 3_{10} -helix that constricts the active site, making an acetylated lysine side chain, but not an acetylated polyamine, too short to reach the active site zinc atom. In *h*HDAC10, these four residues, numbered 21-24, are Pro-Glu-Cys-Glu. Both an E272L HDAC10 mutant and a mutant lacking the two-residue loop insertion were found to have increased HDAC activity and diminished PDAC activity in enzymatic assays. Interestingly, this model suggests that bulky (e.g. **8**) Class IIB inhibitors cannot fit into the constricted binding pocket of HDAC10 without significant movement of the L1 loop. The fact that an E272L mutation alone is sufficient to enable deacetylation of lysines, however, suggests that the L1 loop may have this flexibility.

While we and others have shown that some known HDAC inhibitors bind HDAC10,³⁸⁻⁴⁰ to the best of our knowledge no study dedicated to the development of HDAC10-selective inhibitors has been published. As such, no validated chemical probes are currently available which can be used to pharmacologically investigate the multiple molecular functions of HDAC10 and address questions of HDAC10 target validation in different diseases. Motivated by the scientific need for a quality HDAC10 chemical probe, and intrigued by the unexpected PDAC enzymatic activity of HDAC10, we initiated a program to discover selective HDAC10inhibitors.

RESULTS AND DISCUSSION:

Testing of known substances in two displacement assays reveals unexpectedly potent HDAC10 binding. Although it is known that HDAC10 enzymatic activity is challenging to assay with acetylated lysine substrates,¹² some contract research organizations offer enzymatic profiling of all HDACs, and IC₅₀ values measured in this way against HDAC10 are sometimes reported in the literature. It has also been claimed that residual co-purified Class I HDACs from HDAC preparations of Class IIA HDACs are largely responsible for the activity observed when testing these proteins in acetyl-lysine based enzymatic assays.⁴¹ In light of this claim, and the recent finding that HDAC10 has significant PDAC activity,⁶ we analyzed a selection of literature data, where enzymatic activities across multiple HDAC isozymes were

reported.^{19, 42-49} Interestingly, strong correlations between HDAC10 and Class I HDAC inhibition values were found, while HDAC6 gave a completely distinct activity profile, despite its high sequence homology to HDAC10 as a Class IIB enzyme (Figure 2, Supplementary Figure 1).

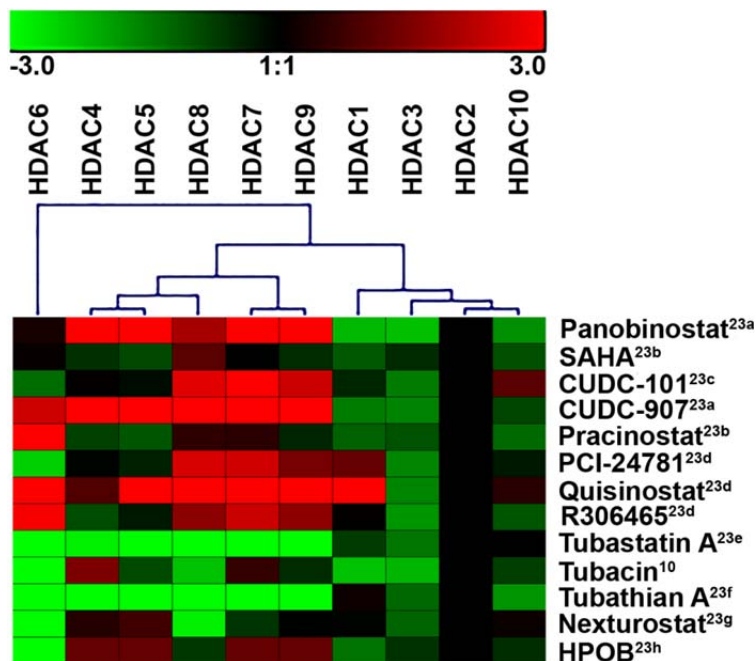


Figure 2. Hierarchical clustering reveals a correlation between HDAC Class I and HDAC10 activities. A selectivity profile of each compound was calculated relative to HDAC2. After log₂ transformation, the values were subjected to hierarchical clustering using the complete-linkage agglomeration rule. Red and green colors indicate higher and lower reported IC₅₀ values, respectively, of a given drug on an HDAC isozyme relative to HDAC2. Superscripts indicate the reference from where the data was taken.

On the basis of this analysis, and due to the low-throughput format of Christianson’s PDAC assay, we decided that it would be prudent to assay HDAC10 in a non-enzymatic format. So as to eliminate any complications that could arise from co-purified HDAC impurities, two ligand displacement assays that employ genetically tagged HDAC proteins for signal generation were utilized, thereby ensuring reliable identification of HDAC10 binders. For screening against pure recombinant HDAC10, a time resolved fluorescence energy transfer (TR-FRET) assay that measures displacement of a fluorescently-labeled ligand was used (Figure 3a).⁵⁰ A conceptually similar bioluminescence energy transfer (BRET) assay was also utilized with cells that overexpress nano-luciferase-tagged HDAC10 (Figure 3b, Supplementary Figure 2).⁵¹ The BRET assay can independently confirm the TR-FRET assay and provides target engagement values in living cells.

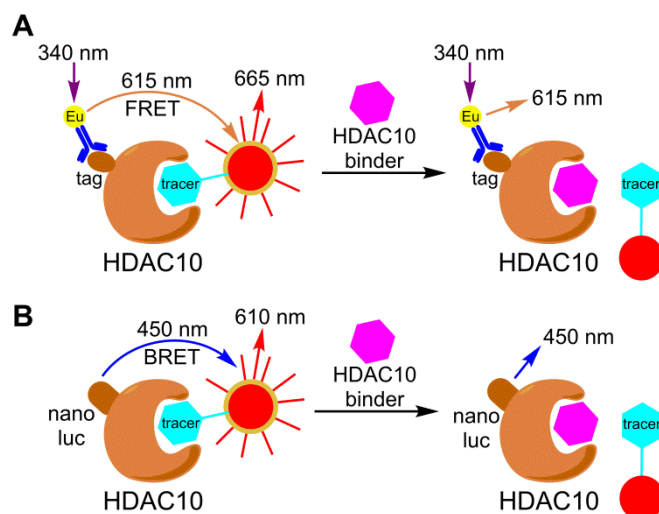


Figure 3: HDAC10 ligand displacement assays. A) TR-FRET assay: A Europium labelled anti-GST tag antibody is coupled to GST-tagged HDAC10 protein. When HDAC10 is bound by a dye-labelled tracer molecule, irradiation with 340 nm light produces productive FRET between the Europium (615 nM emission) and the dye (665 nM emission). In the presence of an HDAC10 binder, which competes with the tracer ligand, FRET is disrupted and a change in the signal is observed. B) BRET assay: When cells expressing nano-luciferase-tagged HDAC10 are treated with a dye-labelled tracer and nano-luciferase substrate, productive BRET is observed. In the presence of an HDAC10 binder, BRET is disrupted.

A series of commercially available HDAC inhibitors, which have been reported to have high HDAC6 activity, were tested in both HDAC10 assays (Table 1, Supplementary Figure 1). Ricolinostat (**10**) showed almost a 10-fold difference in activity between the two assays, but the majority of compounds had pIC_{50} values that were within 0.5 log units of each other. The BRET assay typically gave lower potencies, which can be expected when comparing cellular and biochemical assay formats. It was not surprising that some of the pan-HDAC inhibitor compounds (**2**, **10–15**) showed quite high activity in the HDAC10 displacement assays. Indeed, all of these compounds, except pracinostat (**13**), had sub-micromolar IC_{50} values ($pIC_{50} \geq 6.0$) in at least one of the assays. Most interesting were the results with tubastatin A (**8**) HPOB (**16**)⁵², and nexturastat (**17**)⁵³ compounds that have been described as highly selective HDAC6 inhibitors with poor HDAC10 inhibitory activities. While both HPOB and nexturastat were found to be moderately potent HDAC10 binders, Tubastatin A was active in the low nanomolar range ($pIC_{50} = 7.9$) in both the FRET and BRET assays. A control experiment with PCI-34051, a hydroxamate-containing HDAC8 selective inhibitor, gave low binding values in both assays.

Table 1. TR-FRET biochemical and BRET cellular HDAC10 binding data with commercial inhibitors.

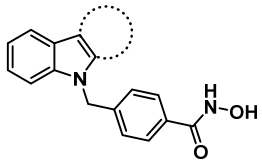
Cmpd.	Substance	HDAC10 FRET pIC ₅₀ ^a	HDAC10 BRET pIC ₅₀ ^b
2	SAHA ^c	6.7	6.2
10	Ricolinostat ^c	6.9	5.8
11	CAY-10603 ^c	6.5	6.1
12	CUDC-101 ^c	6.9	6.4
13	Pracinostat ^c	5.9	5.5
14	Quisinostat ^c	8.0	7.4
15	Abexinostat ^c	8.4	8.1
8	Tubastatin A ^d	7.9	7.9
16	HPOB ^d	7.1	6.5
17	Nexturastat ^d	7.0	6.3
18	PCI-34051 ^e	4.4	<5.0


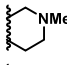
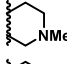
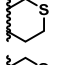
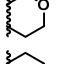
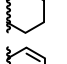
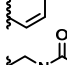
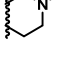
^a FRET pIC₅₀ values are the mean of at least two independent experiments. ^b BRET pIC₅₀ values are calculated from one experiment performed in triplicate. ^c pan-HDAC inhibitor. ^d HDAC6 “selective” inhibitor. ^e HDAC8 selective inhibitor.

Tubastatin A analogs lacking a basic amine in the cap group have diminished HDAC10 binding.

Intrigued by the high potency of the HDAC6-selective inhibitor tubastatin A against HDAC10, we chose to more closely examine the structure–activity relationship (SAR) of the “cap group” with respect to HDAC10 and HDAC6 binding. A targeted selection of tubastatin A cap-group analogs were synthesized and tested in both the TR-FRET and the BRET HDAC10 assays, as well as against HDAC6 in the BRET assay format. As was found with the commercial inhibitors, pIC₅₀ values of the TR-FRET and BRET HDAC10 assays were quite consistent for all compounds assayed (Table 2). More illuminating was the comparison of the HDAC10 and HDAC6 BRET pIC₅₀ values for the various derivatives. Tubastatin A (**8**) gave a pIC₅₀ of 7.9 against HDAC10 and of 7.0 against HDAC6.³⁷⁻³⁸ Tetrahydro-β-carboline **19**,¹⁹ which differs from **8** only in the location of the carboline nitrogen, was found to be roughly an order of magnitude less active than **8** in the two HDAC10 assays, but essentially equipotent in the HDAC6 assay. An even greater drop in HDAC10 activities, relative to **8**, was observed for compounds **20**⁵⁴ and **21**, where the γ-carboline nitrogen of **8** is replaced with sulfur and oxygen atoms, respectively. As with **19**, however, compounds **20** and **21** have only slightly diminished (**20**) or improved (**21**) HDAC6 values in comparison to **8**. Tetrahydrocarbazole **22** and carbazole **23**¹⁹ were over 2 orders of magnitude weaker HDAC10 binders than **8**, but again retained their HDAC6 binding capabilities. The acetylated tubastatin A derivative **24** was also found to have significantly diminished HDAC10 binding, but to be equipotent with tubastatin A (**8**) against HDAC6.

Table 2: HDAC6 and HDAC10 binding values of “fused” tubastatin A analogs



Cmpd.		HDAC10		HDAC6	Selectivity BRET HDAC10/ HDAC6 (fold)
		FRET pIC ₅₀ ^a	BRET pIC ₅₀ ^b	BRET pIC ₅₀ ^b	
8		7.9	7.9	7.0	7.9
19		6.7	6.8	7.2	0.4
20		6.5	6.4	6.9 ^c	0.32
21		6.2	6.0	7.7	0.02
22		6.0	5.6	7.2	0.025
23		5.7	5.4	7.4	0.001
24		6.3	5.7	7.1	0.04

^a pIC₅₀ values are the mean of at least 2 independent measurements. ^b pIC₅₀ values are calculated from pooled data of two biological replicates which were each performed in triplicate. ^c pIC₅₀ value is from one experiment performed in triplicate.

It is apparent that while HDAC6 activity is influenced by changes to the indole-fused ring, most modifications result in substances that are similarly potent, or even more potent, than tubastatin A (**8**). This is consistent with published data for **19**, **20**, and **23**, which are all reported to be potent HDAC6 inhibitors.^{19, 54} In contrast, HDAC10 activity appears to be quite sensitive to modifications of the indole-fused ring. Comparing BRET data for the two enzymes shows that while tubastatin A (**8**) binds HDAC10 better than HDAC6 by almost a factor of 10, **19-24** have low (**19**; 2.5 fold) to high (**23**; 100 fold) preferences for HDAC6 over HDAC10.⁵⁵ This is visually represented with the BRET dose response curves of **8**, **19**, and **21** (Figure 4). A basic nitrogen atom embedded in a tetrahydro- γ -carboline structure, therefore, appears to be a critical feature for potent HDAC10 binding, suggestive of a specific polar interaction in the HDAC10 binding site.

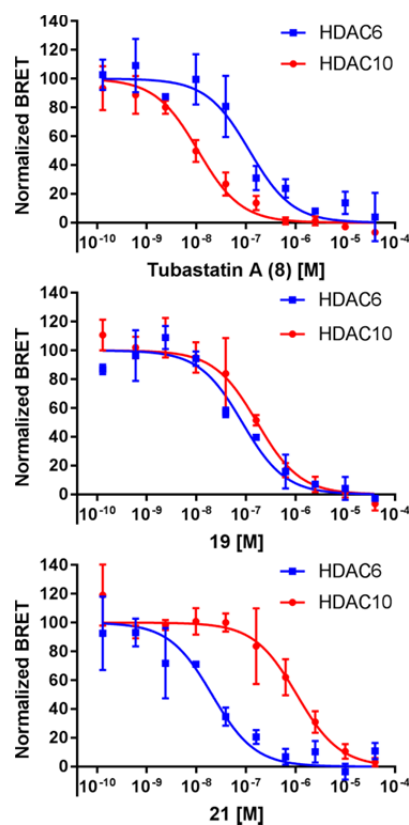
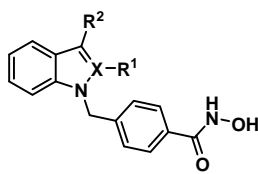


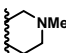
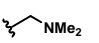
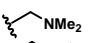
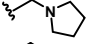
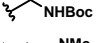
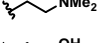
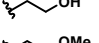
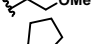
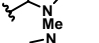
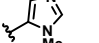
Figure 4: Dose-response curves of compounds **8**, **19**, and **21** in the HDAC6 and HDAC10 BRET assay. Data are from one representative biological replicate that was performed in triplicate. Error bars are standard deviations.

SAR of “Ring-opened” Tubastatin A analogs and HDAC2 selectivity. In order to investigate this hypothesis further, we prepared a series of “ring-opened” tubastatin A analogs, whose structures and binding activities are shown in Table 3. Consistent with our expectations, indole **25** and 2,3-dimethylindole **26** showed diminished activity in both HDAC10 assays, in comparison to **8**. The 2-*tert*-butylindole derivative **27** showed lower activity against both HDAC6 and HDAC10, indicating that the *t*-butyl group is too bulky for either of the two binding pockets. Interestingly, the “re”-introduction of a basic amine into the structure, as in gramine **28**⁵⁶ and pyrrolidine **30**, produced very potent HDAC10 binders, both with BRET pIC₅₀ values of 8.4. Indazole **29**, which is expected to be more pharmacologically stable than **28**, was found to have similar HDAC10 potency to **8**, while Boc-protected amine **31** lost significant HDAC10 binding capacity. Tryptamine **32**⁵⁷ showed good potency against HDAC10 (BRET pIC₅₀ = 7.6), despite the presence of two methylenes between the indole C3 and the nitrogen atom, which was detrimental in the case of **19**. The increased conformational flexibility of ring-opened **32** may allow it to still make a key interaction with the enzyme that **19** cannot. Both the C3 hydroxyethyl (**33**) and methoxyethyl (**34**) derivatives lose almost an order of magnitude binding to HDAC10 in comparison

to **32**, further highlighting the importance of a basic nitrogen in the cap group scaffold. Compound **35**, which incorporates a gramine type structure into a cyclic side chain is also an excellent HDAC10 binder (BRET pIC_{50} = 8.3), while an aromatic imidazole analog (**36**) is 10-fold less potent.

Table 3: HDAC6 and HDAC10 binding/inhibitory values of “ring-opened” Tubastatin A analogs



Cmpd.	X	R ¹	R ²	HDAC10		HDAC6	Selectivity BRET HDAC10/ HDAC6 (fold)
				FRET pIC_{50} ^a	BRET pIC_{50} ^b	BRET pIC_{50} ^b	
8	C			7.9	7.9	7.0	7.9
25	C	H	H	7.2	6.8	7.2	0.4
26	C	Me	Me	6.5	6.2	7.5	0.05
27	C	<i>t</i> -Bu	H	5.3	<4.4	5.7	<0.05
28	C	H		8.3	8.4	6.8	40
29	N	—		7.7	7.8	6.9	7.9
30	C	H		8.4	8.4	6.8	40
31	C	H		6.8	6.6	7.1	0.32
32	C	H		7.7	7.6	6.9	5.0
33	C	H		7.1	6.7	7.5	0.63
34	C	H		6.9	6.7	7.2	0.32
35	C	H		8.3	8.3	6.9	25
36	C	H		7.6	7.3	7.1	1.6

^a pIC_{50} values are the mean of at least 2 independent measurements. ^b pIC_{50} values are calculated from pooled data of two biological replicates which were each performed in triplicate.

As found with the “fused” analogs in Table 1, BRET HDAC6 activity was relatively insensitive to structural changes, with all compounds except *t*-Bu substituted **27** having activities within a single order of magnitude range ($6.8 < pIC_{50} < 7.5$). Amine analogs **28-30**, **32**, and **35** all show activities similar or better than tubastatin A against HDAC10, with moderate selectivity (≥ 0.7 log units) over HDAC6. Compounds **28**, **30**, and **35** appear to have the best profiles in the BRET assays, with pIC_{50} values greater than 8.3 against HDAC10 and selectivities greater than 25 fold against HDAC6.

Selected compounds were also tested in an HDAC2 enzymatic assay to gain insight into their activities against a Class I HDAC enzyme (Table 4). In accordance with the literature, tubastatin A (**8**) had a pIC_{50} of 4.9 (lit. 4.9).⁴⁶ Two other tricyclic-capped derivatives (**19** and **21**) gave values similar to **8** with pIC_{50} s of 4.6 and 5.1, respectively. Due to the relatively large differences between **8**, **19**, and **21** in the

HDAC10 assays, however, selectivity for HDAC10 over HDAC2 ranges from 1000 fold for **8**, to only 13 fold for **21**. HDAC2 potency, relative to **8**, was slightly increased for the ring-opened derivatives **26**, **28**, **29**, and **30**, and somewhat more increased for **35** and **36**. Overall, for those compounds showing potent HDAC10 activity, at least 100 fold selectivity over HDAC2 was retained, with compound **30** showing the highest selectivity difference of 3.2 log units.

Table 4. HDAC2 pIC_{50} values of selected inhibitors.

Cmpd.	pIC_{50} HDAC2 ^a	ΔpIC_{50} (HDAC10 _{FRET} – HDAC2)
8	4.9	3.0
19	4.6	2.1
21	5.1	1.1
26	4.9	1.6
28	5.2	3.1
29	5.1	2.6
30	5.2	3.2
35	5.7	2.6
36	5.5	2.1

^a pIC_{50} values are calculated from one biological replicate performed in triplicate.

Compound HDAC6/10 Inhibition Profiles are Reflected in On-target Activity in Cells. Some selective HDAC10 inhibitors (**8**, **29**, **30**, **35**), some selective HDAC6 inhibitors (**20** and **21**), and one inactive substance (**27**) were also tested in the neuroblastoma BE(2)-C cell line to confirm on-target activity.^{37-38, 40, 58} To test for HDAC6 inhibition, tubulin acetylation was measured by Western blot, and to test for HDAC10 inhibition, expansion of the lysosomal compartment was measured using the pH-dependent LysoTracker DND-99 fluorescent probe. As expected, tubastatin A (**8**) showed a dose-dependent increase in tubulin acetylation (Figure 5A). Substances **20**, **21**, **29**, **30**, and **35** all had profiles similar to **8**, consistent with the fact that they are all similarly potent HDAC6 inhibitors. Only compound **27**, which showed reduced HDAC6 activity in the BRET assay, required higher concentrations to increase tubulin acetylation. In the LysoTracker assay, only those compounds which showed highly potent HDAC10 binding in the BRET and FRET assays (**8**, **29**, **30**, and **35**) strongly induced fluorescence, while **20**, **21**, and **27** gave no to weak increases (Figure 5B).

Homology Modeling Provides a Rationale for Selective HDAC10 Binding. The Glu272 gatekeeper residue is the single determining factor which gives HDAC10 PDAC over HDAC activity.⁶ This selectivity is the result of a polar interaction between the negatively charged glutamic acid and a positively charged

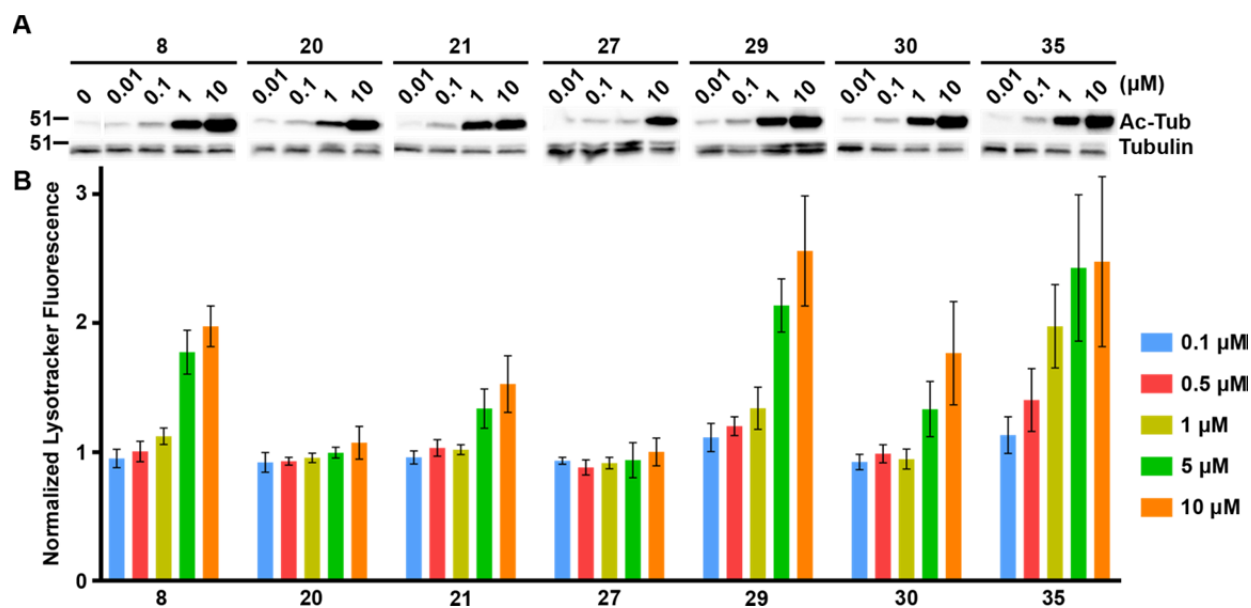


Figure 5. A) Western blot analysis of acetylated tubulin versus total tubulin, as induced by HDAC6 inhibition from tubastatin A (**8**) and analogs. B) Expansion of the lysosomal compartment as a measure of HDAC10 inhibition, shown by increased fluorescence from the LysoTracker DND-99 probe. Data is normalized to the fluorescence measured with only DMSO and represents Mean \pm SD from at least 3 experiments.

polyamine. We wondered whether inhibitors with a basic amine in the cap group were such strong HDAC10 binders due to a similar polar interaction with Glu272. Moreover, highly potent binders such as **8**, **28** and **35** indicate that bulky inhibitors are able to fit into the constricted binding pocket of HDAC10, probably requiring significant movement of the L1 loop. To investigate, we built several different homology models of *h*HDAC10 and performed docking studies. Initially, two *h*HDAC10 homology models were prepared, one based on a crystal structure of *z*HDAC10 (pdb 5td7) and one based on *h*HDAC6 (pdb 5edu), hereafter referred to as Model I and Model II, respectively. Both Model I and Model II were used for docking studies of tubastatin A (**8**). Model I has an L1 loop that closely resembles that of the parent *z*HDAC10 structure, and failed to show any reliable docking poses. Model II has an L1 loop more similar to its parent *h*HDAC6 structure, and showed high-scoring docking poses of **8** with a hydrogen bond to Glu272 (Figure 6A). A superposition of the two models clearly indicated that the L1 loop in Model I prevents binding, as **8** would clash with the L1 loop (Figure 6B). To investigate the loop flexibility that seems to be needed for docking of **8**, two additional models were built. For one of these models (Model III), the ligand of pdb 5edu (trichostatin A (**1**)) was transferred into pdb 5td7 to introduce an induced fit during model building. For the other model (Model IV), residues 14-28 from the L1 loop were removed and rebuilt using MOE's "build loop" module. Both Model III and Model IV resulted in new L1 loop

conformations. Interestingly, docking of **8** into these models succeeded, leading to hydrogen-bonded docking poses similar to what was found in Model II (Figures 6C and 6D). To summarize, in the four models reliable docking poses were only identified when the L1 loop adopted a conformation different from what is found in the zHDAC10 structure, suggesting that flexibility of the L1 loop is needed for tubastatin A binding.

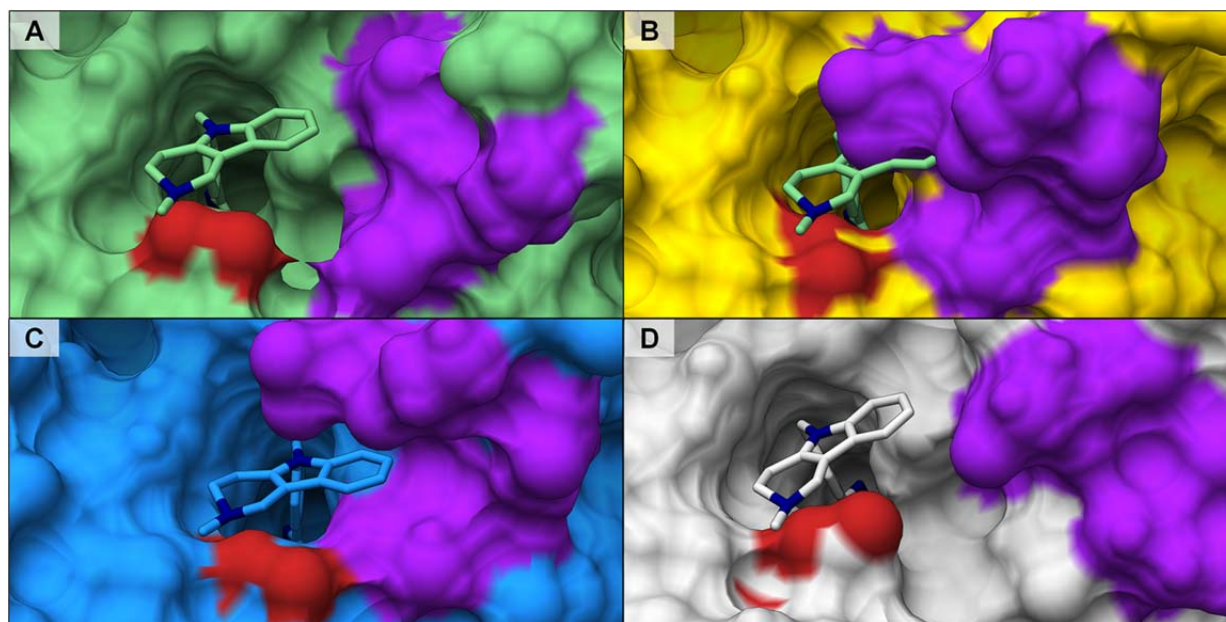


Figure 6: Docking poses of Tubastatin A in hHDAC10 models (red: oxygen of Glu272 as hydrogen bond partner; magenta: L1 loop). A) Model II (green). B) Superposition of **8** docking pose in Model II (green) with Model I (yellow). C) Induced fit Model III. D) Alternative L1 loop Model IV.

Compounds **20**, **21**, and **29** were also docked in the human HDAC10 homology models. The docking poses of **20** and **21** show only hydrophobic interactions in the cap group region, with no polar interactions to Glu272 (Figure 7A), while adopting similar conformations to **8** (Figure 7B). For **20** and **21**, the flexible Glu272 moved beneath the ring system during docking because no hydrogen bonding could occur. This difference in binding between **8** and **20/21** could explain their disparate binding activities. Several possible docking poses were found for **29** in different models, with hydrogen bonding via its dimethylamino group to one of two glutamic acids surrounding the binding site. In Model II, one binding pose with a contact to Glu272 was found (Figure 7C). In Model III, **29** adopted a pose that is almost a mirror image to what was found in Model II (Figure 7D). Intriguingly, another pose for **29** was found with Model III, where the dimethylamino group engages in a hydrogen bond to Glu22, one of the four critical L1 loop residues (vide supra). Here, the homology modelling reaches its limit to provide one reliable

binding pose; however, it indicates that **29** can address at least one of the two glutamic acids in the binding region of HDAC10 (Glu22, Glu272), which are not present in HDAC6.

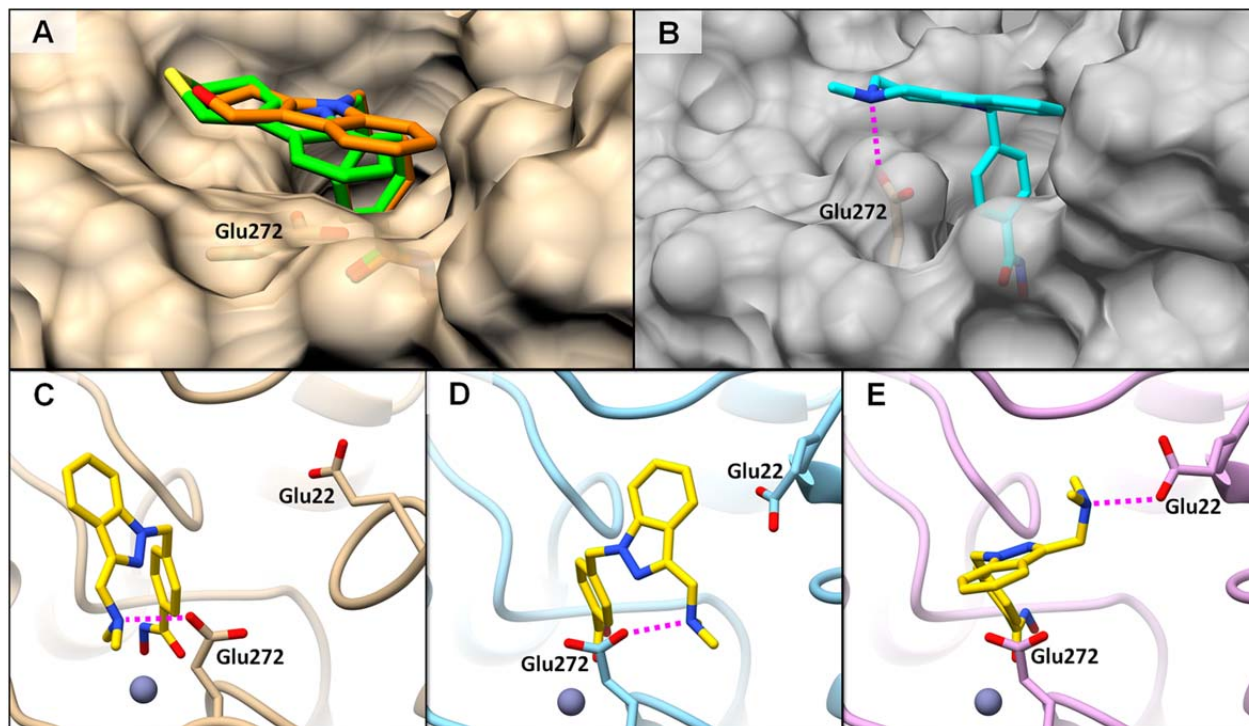


Figure 7: Docking poses of **8**, **20**, **21** and **29** (pink dotted line: hydrogen bond). A) **20** (orange) and **21** (lime green) in Model II (tan). B) **8** (blue) in Model II (gray). C) **29** (gold) in Model II (tan). D) **29** (gold) bound to Glu272 in Model IV (blue). E) **29** (gold) bound to Glu22 in Model IV (pink).

Tubastatin A (**8**), **20**, **21**, and **29** were also docked into *h*HDAC6 (5edu), giving one main binding pose for all four substances and one alternative binding mode for all except **29**. These docking poses show largely hydrophobic interactions of the cap groups with HDAC6, consistent with the fact that the structural differences between the compounds do not have dramatic effects on HDAC6 binding in the BRET assay.

CONCLUSIONS

The use of complementary TR-FRET and BRET HDAC10 displacement assays has enabled the discovery that a number of well-known HDAC inhibitors are capable of potently binding HDAC10. Moreover, substances which have previously been described as being highly selective HDAC6 inhibitors, with little to no HDAC10 activity (e.g. tubastatin A (**8**), HPOB (**16**), nexturastat (**17**)) have also been found to be good HDAC10 binders. We investigated SAR surrounding the indole-fused ring of **8**, and found a strong dependency for HDAC10 binding on the presence of an appropriately placed basic amine

functionality. In contrast, no dependency on such a functional group was observed for HDAC6 binding. Compounds, such as **28** and **35**, with high HDAC10 potency, good selectivity over HDAC6, and high selectivity over HDAC2 were discovered. The TR-FRET and BRET HDAC10 assay data was supported by monitoring acetylation levels of tubulin (HDAC6 substrate) and expansion of the lysosomal compartment (HDAC10 inhibition phenotype) in inhibitor-treated cells. Furthermore, docking of selected inhibitors into an HDAC6 X-ray crystal structure as well as into four different HDAC10 homology models provided a structural rationale for our experimental observations. The modeling suggests that derivatives of tubastatin A make largely hydrophobic interactions with HDAC6 regardless of the presence or absence of a basic amine in the cap group scaffold. On the other hand, derivatives with an appropriately placed amino exhibit increased binding via a hydrogen bond with the gatekeeper residue Glu272 (and potentially Glu22) of HDAC10. At the same time, the L1 loop of HDAC10 must exhibit some flexibility to accommodate these inhibitors. During the preparation of this manuscript, another homology model of *h*HDAC10, based on the *z*HDAC10 structure, was reported.⁵⁹ Docking of well-known HDAC inhibitors was shown, but an adapted L1 loop conformation seemed not to be required.

Taken together, the TR-FRET, BRET, LysoTracker, and modeling data strongly support that the L1 Loop is flexible enough to accommodate “bulky” inhibitors like **8**, **28**, and **35**.⁶⁰ Consistent with our data is a model where HDAC10 adopts the narrow conformation found in the X-ray structure of the zebrafish HDAC10 enzyme, and, in conjunction with the gatekeeper residue, is responsible for HDAC10 PDAC activity. Having some flexibility, the L1 loop can also adopt an open conformation, which still doesn’t effectively process acetylated lysines due to the gatekeeper residue, but which conformationally resembles HDAC6 and can be engaged by HDAC inhibitors. Substances containing cap groups that bind HDAC6 *and* are capable of hydrogen bonding to gatekeeper residue Glu272 become particularly potent HDAC10 inhibitors.

The work described herein provides a means to tune HDAC10 binding activity. When working with a scaffold that already exhibits high selectivity over Class I and IIA HDAC enzymes (e.g. tubastatin A), it is possible to discover potent and selective HDAC10 inhibitors. In order to develop a highly selective HDAC10 chemical probe, however, one must be able to modulate HDAC6 activity. So far we have been unable to abolish HDAC6 activity while retaining HDAC10 activity when working with the tubastatin A scaffold. This is perhaps not surprising as there appears to be significant flexibility in size and composition of the cap group when making selective HDAC6 inhibitors.⁶¹ Progress to realize the goal of a true HDAC10-selective inhibitor will be the subject of future reports.

SUPPORTING INFORMATION

Supplementary figures, experimental procedures, compound synthesis, characterization data, and ¹H and ¹³C NMR spectra of newly synthesized substances (**21**, **22**, **24**, **27**, **29**, **30**, **31**, **33**, **34**, **35**, and **36**).

AUTHOR INFORMATION

Corresponding Author

* aubry.miller@dkfz.de

ORCID

Aubry K. Miller: 0000-0002-1761-4143

Oliver Koch: 0000-0001-9228-217X

Present Address

M.G. Develco Pharma, Schopfheim, Germany

Author Contributions

All authors have given approval to the final version of the manuscript.

Notes

The authors declare no competing financial interests.

ACKNOWLEDGMENT

Financial support from the Helmholtz Drug Initiative and the German Cancer Consortium (DKTK) is gratefully acknowledged. We thank Dr. Matt Robers of Promega for support and advice in the utilization of the BRET assay, Johanna Hummel-Eisenbeiß for establishment of the HDAC6 and HDAC10 stable clones, and Jasmin Lohbeck and Ulrike Wagner for chemical synthesis support. We thank Dr. Karel Klika and Gabriele Schwebel for NMR spectroscopy support. Protein X-ray graphics and analyses were performed with the UCSF Chimera package. Chimera is developed by the Resource for Biocomputing, Visualization, and Informatics at the University of California, San Francisco (supported by NIGMS P41-GM103311).

References and Notes

- (1) Taunton, J., et al. A mammalian histone deacetylase related to the yeast transcriptional regulator Rpd3p. *Science* **1996**, *272*, 408-411.
- (2) Marks, P. A.; Breslow, R. Dimethyl sulfoxide to vorinostat: development of this histone deacetylase inhibitor as an anticancer drug. *Nat. Biotechnol.* **2007**, *25*, 84-90.

- (3) Falkenberg, K. J.; Johnstone, R. W. Histone deacetylases and their inhibitors in cancer, neurological diseases and immune disorders. *Nat. Rev. Drug Disc.* **2014**, *13*, 673-691.
- (4) Roche, J.; Bertrand, P. Inside HDACs with more selective HDAC inhibitors. *Eur. J. Med. Chem.* **2016**, *121*, 451-483.
- (5) Kutil, Z., et al. Histone deacetylase 11 is a fatty-acid deacylase. *ACS Chem. Biol.* **2018**, *13*, 685-693.
- (6) Hai, Y., et al. Histone deacetylase 10 structure and molecular function as a polyamine deacetylase. *Nat. Commun.* **2017**, *8*, 15368.
- (7) Aramsangtienchai, P., et al. HDAC8 catalyzes the hydrolysis of long chain fatty acyl lysine. *ACS Chem. Biol.* **2016**, *11*, 2685-2692.
- (8) Feldman, J. L., et al. Activation of the protein deacetylase SIRT6 by long-chain fatty acids and widespread deacylation by mammalian sirtuins. *J. Biol. Chem.* **2013**, *288*, 31350-31356.
- (9) Moreno-Yruela, C., et al. Histone Deacetylase 11 Is an ϵ -N-Myristoyllysine Hydrolase. *Cell Chem. Biol.* **2018**, *25*, 849-856.
- (10) Witt, O., et al. HDAC family: What are the cancer relevant targets? *Cancer Lett.* **2009**, *277*, 8-21.
- (11) Balasubramanian, S., et al. Isoform-specific histone deacetylase inhibitors: The next step? *Cancer Lett.* **2009**, *280*, 211-221.
- (12) Bradner, J. E., et al. Chemical phylogenetics of histone deacetylases. *Nat. Chem. Biol.* **2010**, *6*, 238-243.
- (13) Boskovic, Z. V., et al. Inhibition of zinc-dependent histone deacetylases with a chemically triggered electrophile. *ACS Chem. Biol.* **2016**, *11*, 1844-1851.
- (14) Lobera, M., et al. Selective class IIa histone deacetylase inhibition via a nonchelating zinc-binding group. *Nat. Chem. Biol.* **2013**, *9*, 319-325.
- (15) Mai, A., et al. Class II (IIa)-selective histone deacetylase inhibitors. 1. Synthesis and biological evaluation of novel (aryloxopropenyl)pyrrolyl hydroxyamides. *J. Med. Chem.* **2005**, *48*, 3344-3353.
- (16) Martin, M. W., et al. Discovery of novel N-hydroxy-2-arylisoindoline-4-carboxamides as potent and selective inhibitors of HDAC11. *Bioorg. Med. Chem. Lett.* **2018**, *28*, 2143-2147.
- (17) Marek, L., et al. Histone deacetylase (HDAC) inhibitors with a novel connecting unit linker region reveal a selectivity profile for HDAC4 and HDAC5 with improved activity against chemoresistant cancer cells. *J. Med. Chem.* **2013**, *56*, 427-436.
- (18) Haggarty, S. J., et al. Domain-selective small-molecule inhibitor of histone deacetylase 6 (HDAC6)-mediated tubulin deacetylation. *Proc. Nat. Acad. Sci.* **2003**, *100*, 4389-4394.
- (19) Butler, K. V., et al. Rational design and simple chemistry yield a superior, neuroprotective HDAC6 inhibitor, tubastatin A. *J. Am. Chem. Soc.* **2010**, *132*, 10842-10846.
- (20) Jochems, J., et al. Antidepressant-like properties of novel HDAC6-selective inhibitors with improved brain bioavailability. *Neuropsychopharmacology* **2013**, *39*, 389-400.
- (21) Arrowsmith, C. H., et al. The promise and peril of chemical probes. *Nat. Chem. Bio.* **2015**, *11*, 536-541.
- (22) Fischer, D. D., et al. Isolation and characterization of a novel class II histone deacetylase, HDAC10. *J. Biol. Chem.* **2002**, *277*, 6656-6666.
- (23) Guardiola, A. R.; Yao, T. P. Molecular cloning and characterization of a novel histone deacetylase HDAC10. *J. Biol. Chem.* **2002**, *277*, 3350-3356.
- (24) Kao, H. Y., et al. Isolation and characterization of mammalian HDAC10, a novel histone deacetylase. *J. Biol. Chem.* **2002**, *277*, 187-193.
- (25) Lai, I. L., et al. Histone deacetylase 10 relieves repression on the melanogenic program by maintaining the deacetylation status of repressors. *J. Biol. Chem.* **2010**, *285*, 7187-7196.
- (26) Park, B. L., et al. HDAC10 promoter polymorphism associated with development of HCC among chronic HBV patients. *Biochem. Biophys. Res. Commun.* **2007**, *363*, 776-781.
- (27) Kotian, S., et al. Histone deacetylases 9 and 10 are required for homologous recombination. *J. Biol. Chem.* **2011**, *286*, 7722-7726.

- (28) Park, J. H., et al. Class II histone deacetylases play pivotal roles in heat shock protein 90-mediated proteasomal degradation of vascular endothelial growth factor receptors. *Biochem. Biophys. Res. Commun.* **2008**, *368*, 318-322.
- (29) Jin, Z., et al. Decreased expression of histone deacetylase 10 predicts poor prognosis of gastric cancer patients. *Int. J. Clin. Exp. Pathol.* **2014**, *7*, 5872-5879.
- (30) Osada, H., et al. Reduced expression of class II histone deacetylase genes is associated with poor prognosis in lung cancer patients. *International journal of cancer* **2004**, *112*, 26-32.
- (31) Powers, J., et al. Expression and function of histone deacetylase 10 (HDAC10) in B cell malignancies. *Methods in molecular biology* **2016**, *1436*, 129-145.
- (32) Song, C., et al. Histone deacetylase (HDAC) 10 suppresses cervical cancer metastasis through inhibition of matrix metalloproteinase (MMP) 2 and 9 expression. *J. Biol. Chem.* **2013**, *288*, 28021-28033.
- (33) Fan, W., et al. Histone deacetylase 10 suppresses proliferation and invasion by inhibiting the phosphorylation of beta-catenin and serves as an independent prognostic factor for human clear cell renal cell carcinoma. *Int. J. Clin. Exp. Med.* **2015**, *8*, 3734-3742.
- (34) Islam, M. M., et al. HDAC10 as a potential therapeutic target in ovarian cancer. *Gynecol. Oncol.* **2017**, *144*, 613-620.
- (35) Oehme, I., et al. Histone deacetylase 10-promoted autophagy as a druggable point of interference to improve the treatment response of advanced neuroblastomas. *Autophagy* **2013**, *9*, 2163-2165.
- (36) Yang, Y., et al. HDAC10 promotes lung cancer proliferation via AKT phosphorylation. *Oncotarget* **2016**, *7*, 59388-59401.
- (37) Oehme, I., et al. Histone deacetylase 10 promotes autophagy-mediated cell survival. *Proc. Nat. Acad. Sci.* **2013**, *110*, E2592-E2601.
- (38) Ridinger, J., et al. Dual role of HDAC10 in lysosomal exocytosis and DNA repair promotes neuroblastoma chemoresistance. *Sci. Rep.* **2018**, *8*, 10039.
- (39) Bantscheff, M., et al. Chemoproteomics profiling of HDAC inhibitors reveals selective targeting of HDAC complexes. *Nat. Biotechnol.* **2011**, *29*, 255-265.
- (40) Kolbinger, F. R., et al. The HDAC6/8/10 inhibitor TH34 induces DNA damage-mediated cell death in human high-grade neuroblastoma cell lines. *Arch. Toxicol.* **2018**, *92*, 2649-2664.
- (41) Jones, P., et al. Probing the elusive catalytic activity of vertebrate class IIa histone deacetylases. *Bioorg. Med. Chem. Lett.* **2008**, *18*, 1814-1819.
- (42) Qian, C., et al. Cancer network disruption by a single molecule inhibitor targeting both histone deacetylase activity and phosphatidylinositol 3-kinase signaling. *Clin. Cancer Res.* **2012**, *18*, 4104-4113.
- (43) Novotny-Diermayr, V., et al. SB939, a novel potent and orally active histone deacetylase inhibitor with high tumor exposure and efficacy in mouse models of colorectal cancer. *Mol. Cancer Ther.* **2010**, *9*, 642-652.
- (44) Lai, C. J., et al. CUDC-101, a multitargeted inhibitor of histone deacetylase, epidermal growth factor receptor, and human epidermal growth factor receptor 2, exerts potent anticancer activity. *Cancer Res.* **2010**, *70*, 3647-3656.
- (45) Arts, J., et al. JNJ-26481585, a novel "second-generation" oral histone deacetylase inhibitor, shows broad-spectrum preclinical antitumoral activity. *Clin. Cancer Res.* **2009**, *15*, 6841-6851.
- (46) Shen, S., et al. Bicyclic-capped histone deacetylase 6 inhibitors with improved activity in a model of axonal Charcot–Marie–tooth disease. *ACS Chem. Neurosci.* **2016**, *7*, 240-258.
- (47) De Vreese, R., et al. Synthesis and SAR assessment of novel tubathian analogs in the pursuit of potent and selective HDAC6 inhibitors. *Org. Biomol. Chem.* **2016**, *14*, 2537-2549.
- (48) Sotomayor, E. M., et al. Selective Histone Deactylase 6 Inhibitors. WO2013134467 A1, 2013.
- (49) Lee, J. H., et al. Development of a histone deacetylase 6 inhibitor and its biological effects. *Proc. Natl. Acad. Sci. U.S.A.* **2013**, *110*, 15704-15709.
- (50) Marks, B. D., et al. A substrate-independent TR-FRET histone deacetylase inhibitor assay. *J. Biomol. Screen.* **2011**, *16*, 1247-1253.

- (51) Robers, M. B., et al. Target engagement and drug residence time can be observed in living cells with BRET. *Nat. Commun.* **2015**, *6*, 10091.
- (52) Lee, J. H., et al. Development of a histone deacetylase 6 inhibitor and its biological effects. *Proc. Natl. Acad. Sci. USA* **2013**, *110*, 15704-15709.
- (53) Bergman, J. A., et al. Selective histone deacetylase 6 inhibitors bearing substituted urea linkers inhibit melanoma cell growth. *J. Med. Chem.* **2012**, *55*, 9891-9899.
- (54) De Vreese, R., et al. Potent and selective HDAC6 inhibitory activity of N-(4-hydroxycarbamoylbenzyl)-1,2,4,9-tetrahydro-3-thia-9-azafluorenes as novel sulfur analogues of tubastatin A. *Chem. Comm.* **2013**, *49*, 3775-3777.
- (55) pIC50 values against the two enzymes should be directly comparable because the BRET tracer ligand has been shown to have almost identical KD values with HDAC6 and HDAC10. See reference 25.
- (56) Nepali, K., et al. Ring-opened tetrahydro-gamma-carbolines display cytotoxicity and selectivity with histone deacetylase isoforms. *Eur. J. Med. Chem.* **2017**, *127*, 115-127.
- (57) Kozikowski, A., et al. Preparation Of 4-Substituted N-Hydroxybenzamides as HDAC Inhibitors And Therapeutic Methods Using Them. WO2012106343A2, 2012.
- (58) Hubbert, C., et al. HDAC6 is a microtubule-associated deacetylase. *Nature* **2002**, *417*, 455-458.
- (59) Uba, A. I.; Yelekçi, K. Homology modeling of human histone deacetylase 10 and design of potential selective inhibitors. *J. Biomol. Struct. Dyn.* Ahead of print; DOI: 10.1080/07391102.2018.1521747.
- (60) Tubastatin A and HPOB inhibit human HDAC10 PDAC activity; personal communication from D. Christianson.
- (61) Leonhardt, M., et al. Design and biological evaluation of tetrahydro-beta-carboline derivatives as highly potent histone deacetylase 6 (HDAC6) inhibitors. *Eur. J. Med. Chem.* **2018**, *152*, 329-357.